

Small-Signal Characterization of FET/HEMT for Terahertz Applications

E. STARIKOV^a, P. SHIKTOROV^a, V. GRUŽINSKIS^a, H. MARINCHIO^b, P. NOUVEL^b,
J. TORRES^b, C. PALERMO^b, L. CHUSSEAU^b, L. VARANI^b AND P. ZIADÉ^c

^aSemiconductor Physics Institute, Center for Physical Sciences and Technology
A. Goštauto 11, LT-01108, Vilnius, Lithuania

^bInstitut d'Electronique du Sud (CNRS UMR 5214), Université Montpellier 2
Place Eugène Bataillon, 34095 Montpellier Cedex 5, France

^cLaboratoire De Physique Appliquée, Faculté des Sciences II, Université Libanaise, Fanar, Lebanon

Calculations of the small-signal response of InGaAs HEMTs by using the hydrodynamic approach coupled with a pseudo-2D Poisson equation are performed. The spectra of small-signal admittance and impedance are found to demonstrate series of the resonant peaks corresponding to excitation of plasma waves. Possibilities and conditions of instability onset and THz signal detection are discussed.

PACS: 72.20.Ht, 72.30.+q

1. Introduction

In recent years significant attention has been paid to the physical processes responsible for electron transport in modern field effect transistor (FET) and high electron mobility transistor (HEMT) channels. The final goal is to use them for various terahertz (THz) applications. For this sake the effects related to the excitation of two-dimensional (2D) plasma waves are considered as the most interesting phenomena at the moment. On the one hand, 2D plasma oscillations can lead to THz radiation emission and/or generation due to various plasma instabilities (for example, the so-called Dyakonov–Shur instability [1]). On the other hand, the excitation of 2D plasma waves can be used for THz signal detection which was recently observed experimentally in sub- and near-THz regions (see, e.g. [2] and references therein). Of course, for the analysis of the conditions favourable to realize these effects the knowledge of the small-signal admittance and impedance of FET/HEMT structures interesting for THz applications is of great importance.

The aim of this work is just to perform such an investigation through the calculation of the small-signal response of InGaAs HEMTs by using the hydrodynamic approach coupled with a pseudo-2D Poisson equation [2, 3].

2. Numerical results

Below we shall present hydrodynamic calculations of small-signal characteristics of HEMT structure based on 50–500–50 nm n^+nn^+ In_{0.53}Ga_{0.47}As channel with the width $\delta = 15$ nm. 400 nm gate is centered in n -region at a

distance $d = 15$ nm from the channel. $n = 8 \times 10^{17}$ cm⁻³, $n^+ = 4 \times 10^{18}$ cm⁻³. The momentum relaxation rate equal to 2×10^{12} s⁻¹ is assumed.

It is supposed that the gate is directly connected with the source by wire so that a perturbation can be applied to source-drain or gate-drain circuits only. In the general case the small-signal current response δj_l at a terminal l is linearly related with the voltage perturbation δU_m at the terminal m through elements of the Y (admittance) matrix: $\delta j_l = Y_{lm}\delta U_m$. The reverse relation is usually represented by the impedance matrix Z as: $\delta U_l = Z_{lm}\delta j_m$. Following Ref. [4] we shall put $l, m = 1$ for the gate and $l, m = 2$ for the drain, respectively. Since we are interested mainly in 2D-plasma-wave effects originating from carrier propagation along the channel the ac behavior of the drain current (voltage) response to the ac small-signal voltage (current) perturbation at the drain contact is of the most importance. In above notions it is represented by drain-related diagonal components Y_{22} and Z_{22} of admittance and impedance matrix. To obtain small-signal spectra of these quantities we are using the Fourier transform of transient response of drain current (or voltage) to voltage (or current) step perturbation at the drain terminal (see, e.g. [4] for more details).

2.1. 2D-plasma resonances

Let us recall once more that the inherent feature of FETs/HEMTs is an excitation of standing plasma waves in the conducting channel as a response to any internal or external perturbations [3]. As a consequence, in the response spectrum there appears a series of resonant

peaks corresponding to frequencies of eigen spatial modes of plasma waves. It should be stressed that the fundamental spatial mode depends on the operation regime of FET/HEMT formulated usually as either the constant voltage or the constant current applied at the drain terminal. Correspondingly, the fundamental spatial mode is defined as $\lambda/2 = L_g$ and $\lambda/4 = L_g$ for the drain voltage- and current-driven operations, respectively [3]. Here L_g is the length of a gated region of HEMT channel, and λ is the plasma wavelength. As follows from the above equations in the former case the fundamental frequency is twice higher than in the latter one.

This is illustrated by Fig. 1 which shows the frequency dependence of the small-signal admittance and impedance real parts, $\text{Re}[Y(f)]$ and $\text{Re}[Z(f)]$, respectively, calculated directly by using the time response of the drain current (or voltage), $\Delta j_d(t)$ (or $\Delta U_{ds}(t)$) to step-like voltage (or current) perturbation, ΔU_{ds} (or Δj_d) applied additionally to the drain terminal at time moment $t = 0$ [4]. Two series of resonant peaks caused by excitation of 2D plasma waves inherent to the constant-voltage and constant-current operations of the HEMT channel at the drain terminal are evident. In the former case, all the resonances $f(k) = kf_I$ ($k = 0, 1, 2, 3, \dots$) of the fundamental plasma frequency $f_I \sim s/2L_g$ of the voltage-driven operation (with s being the plasma wave velocity) manifest itself in the spectrum. In the latter case, only the odd resonances $f(k) = kf_{II}$ ($k = 1, 3, 5, \dots$) of the fundamental plasma frequency $f_{II} \approx f_I/2 \sim s/4L_g$ of the current-driven operation give main contribution into the spectrum.

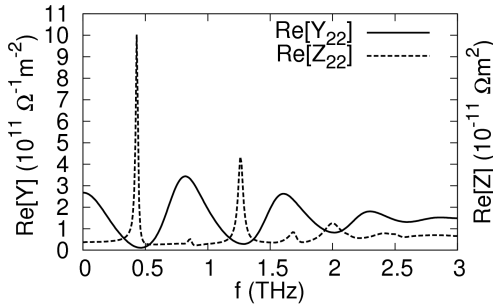


Fig. 1. Frequency dependence of real parts of the small-signal admittance and impedance, $Y_{22}(f)$ and $Z_{22}(f)$, respectively at the drain terminal of the HEMT channel. $U_{ds} = 0.16$ V. $U_g = 0$ V.

The structure of response spectra and their changes with variation of applied voltages (U_{ds} and U_g) will determine a behavior of the HEMT response to various external influences.

2.2. Drain voltage self-oscillations

Figure 2 presents variations of $\text{Re}[Y(f)]$ with increase of U_{ds} . As a general trend, in going from near-linear current-voltage relation (CVR) at low applied voltages to nearly saturated CVR at high U_{ds} a number of well

distinguished resonances decreases as well as an average value of low-frequency $\text{Re}[Y]$ decreases by definition, too. A further scenario depends of the quality of resonances determined by the momentum relaxation rate ν . If ν is sufficiently high (for the structure considered here it is of about $\nu \approx 3 \times 10^{12} \text{ s}^{-1}$ which corresponds to lattice temperature of the bulk material of about 300 K) the admittance real part remains positive everywhere. With reduction of the momentum relaxation rate (e.g. due to lattice temperature decrease) down to values of $\nu \approx 2 \times 10^{12} \text{ s}^{-1}$ and less the quality of the resonant minimum becomes sufficient for a general reduction of low-frequency value of $\text{Re}[Y]$ to result in appearance of negative values of $\text{Re}[Y(f)]$ in the frequency region of first resonant minimum (see Fig. 2). Comparing with Fig. 1 one can conclude that such a behavior of $\text{Re}[Y(f)]$ must result in appearance of self-oscillations of the drain voltage at the fundamental frequency corresponding to the current-driven operation.

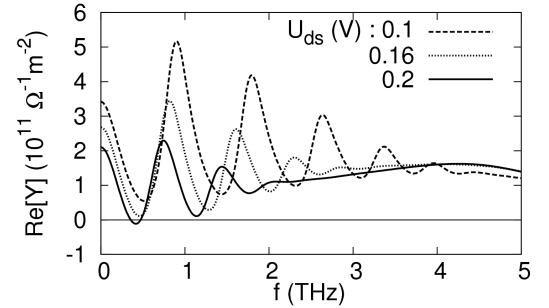


Fig. 2. Frequency dependence of real part of the small-signal admittance at the drain terminal of the HEMT channel calculated under increasing values of drain-to-source voltage U_{ds} . $U_g = 0$ V.

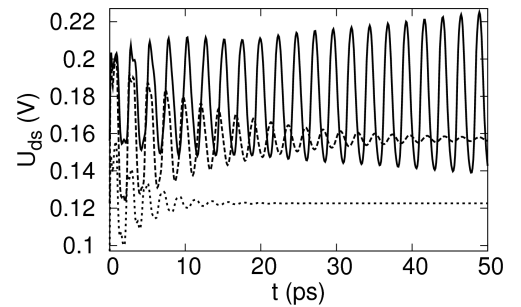


Fig. 3. Transient $U_{ds}(t)$ voltage response calculated for HEMT structure under constant total drain current operation j_d by HD approach with velocity relaxation rate $\nu = 2 \text{ (ps)}^{-1}$. Short- and long-dashed and solid lines correspond, respectively, to $j_d = 50, 60$ and $65 \times 10^9 \text{ A/m}^2$ (U_{ds} , respectively, of 0.12, 0.16 and 0.18 V).

This is illustrated in Fig. 3 which presents time dependence of the drain-voltage response on the step-like perturbation of the drain current from lower to higher

values. Below the threshold drain-current value $j_d^{\text{th}} \approx 62\text{--}63 \times 10^9 \text{ A/m}^2$ for the instability to start the voltage response quickly relaxes to steady-state value of U_{ds} (see short-dashed curve for $j_d = 50 \times 10^9 \text{ A/m}^2$). Approaching to the threshold current j_d^{th} the relaxation becomes longer and longer (see long-dashed curve in Fig. 3 calculated practically just below the threshold). Finally, with the onset of an instability, $U_{ds}(t)$ goes to periodic self-oscillations (see solid line in Fig. 3) with the frequency which well agrees with the instability region predicted by negative values of $\text{Re}[Y(f)]$.

2.3. Detection of THz signal

The idea of a THz signal detection in HEMTs is based on two main assumptions:

(i) an external THz signal appearing inside HEMT channel originates 2D-plasma waves, which, in principle, can lead to THz radiation emission at odd harmonics,

(ii) due to nonlinearity of current–voltage relation the induced 2D-plasma waves can lead to resonant enhancement of the drain-voltage response at zero frequency which can be used for the THz signal detection.

Usually, such a situation is realized by carrier photoexcitation in the HEMT channels induced at the beating frequency of two cw-lasers (see, e.g. [2] and references therein).

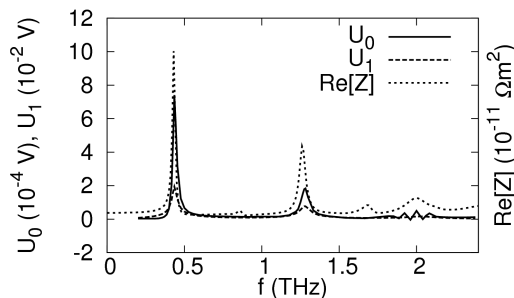


Fig. 4. Frequency response of the drain voltage at the zeroth and first harmonics of the applied beating THz signal. $j_d = 60 \times 10^9 \text{ A/m}^2$.

Figure 4 illustrates a frequency behavior of the drain-voltage response at the zeroth and first harmonics, U_0

and U_1 , respectively, as functions of the beating frequency of photoexcitation. For comparison, short-dashed line shows the frequency dependence of $\text{Re}[Z(f)]$ of the unperturbed HEMT. It is evident that the most pronounced response takes place at the first and third harmonics of the current-operation 2D-plasma wave fundamental frequency.

3. Conclusions

It is shown that the series of resonant peaks corresponding to frequencies of eigen spatial modes of plasma waves excited in HEMT channels under the voltage- and current-driven operations appear in the small-signal admittance and impedance matrix, respectively. It is found that for sufficiently low value of the velocity relaxation rate the small-signal admittance drain-component Y_{22} can reach negative values corresponding to instability onset under constant drain current operation. The maxima of the detection signal and excited plasma response coincide with maxima of the small-signal impedance drain component.

Acknowledgments

This work was supported by grant No. MIP-87/2010 of Lithuanian Science Council.

References

- [1] M. Dyakonov, M. Shur, *Phys. Rev. Lett.* **71**, 2465 (1993).
- [2] P. Nouvel, H. Marinchio, J. Torres, C. Palermo, D. Gasquet, L. Chusseau, L. Varani, P. Shiktorov, E. Starikov, V. Gružinskis, *J. Appl. Phys.* **106**, 013717 (2009).
- [3] P. Shiktorov, E. Starikov, V. Gružinskis, L. Varani, G. Sabatini, H. Marinchio and L. Reggiani, *J. Stat. Mech.: Theory Exp.* **01**, 01047 (2009).
- [4] T. Gonzalez, D. Pardo, *IEEE Trans. Electr. Dev.* **42**, 605 (1995).